



# CHORUS

This is the accepted manuscript made available via CHORUS. The article has been published as:

Large-scale calculations of the double- $\beta$  decay of  $^{76}\text{Ge}$ ,  $^{130}\text{Te}$ ,  $^{136}\text{Xe}$ , and  $^{150}\text{Nd}$  in the deformed self-consistent Skyrme quasiparticle random-phase approximation

M. T. Mustonen and J. Engel

Phys. Rev. C **87**, 064302 — Published 5 June 2013

DOI: [10.1103/PhysRevC.87.064302](https://doi.org/10.1103/PhysRevC.87.064302)

# Large-Scale Calculations of the Double-Beta Decay of $^{76}\text{Ge}$ , $^{130}\text{Te}$ , $^{136}\text{Xe}$ , and $^{150}\text{Nd}$ in the Deformed Self-Consistent Skyrme Quasiparticle Random-Phase Approximation

M. T. Mustonen<sup>1,2,\*</sup> and J. Engel<sup>1,†</sup>

<sup>1</sup>*Department of Physics and Astronomy, CB 3255,*

*University of North Carolina, Chapel Hill, NC 27599-3255*

<sup>2</sup>*Department of Physics, Central Michigan University, Mount Pleasant, MI 48859*

## Abstract

We use the axially-deformed Skyrme Quasiparticle Random-Phase Approximation (QRPA) together with the SkM\* energy-density functional, both as originally presented and with the time-odd part adjusted to reproduce the Gamow-Teller resonance energy in  $^{208}\text{Pb}$ , to calculate the matrix elements governing the neutrinoless double-beta decay of  $^{76}\text{Ge}$ ,  $^{130}\text{Te}$ ,  $^{136}\text{Xe}$ , and  $^{150}\text{Nd}$ . Our matrix elements in  $^{130}\text{Te}$  and  $^{136}\text{Xe}$  are significantly smaller than those of previous QRPA calculations, primarily because of the difference in pairing or deformation between the initial and final nuclei. In  $^{76}\text{Ge}$  and  $^{150}\text{Nd}$  our results are similar to those of less computationally intensive QRPA calculations. We suspect the  $^{76}\text{Ge}$  result, however, because we are forced to use a spherical ground-state, even though our mean-field theory indicates a deformed minimum.

PACS numbers: 21.60.Jz, 23.40.Hc

Keywords: double beta decay, deformed quasiparticle random phase approximation

---

\* mika.t.mustonen@unc.edu

† engelj@physics.unc.edu

## I. INTRODUCTION

Neutrinoless ( $0\nu\beta\beta$ ) double-beta decay can occur if neutrinos are Majorana particles, at a rate that depends on a weighted average of neutrino masses (see Refs. [1, 2] for reviews). The experimental search for  $0\nu\beta\beta$  is approaching sensitivity to neutrino masses below 100 meV [3]. Extracting a mass from the results, however, or setting a reliable upper limit, will require accurate values of the nuclear matrix elements governing the decay, matrix elements that cannot be measured and must therefore be calculated. A number of theorists have attempted the calculations, applying several distinct methods. Among the most popular is the proton-neutron quasiparticle random phase approximation (QRPA).

The QRPA can be carried out at various levels of sophistication. So far, with only a few exceptions [4–9], the mean-fields on which the QRPA is based have been spherical by fiat; most of those which allow deformation have restricted themselves to single-beta decay or two-neutrino double-beta ( $2\nu\beta\beta$ ) decay. And while many employ a kind of self-consistent QRPA [10–12], only Ref. [13] has carried out the QRPA without the use of an artificially inert core, and there again the calculation (which was relativistic) was restricted to  $2\nu\beta\beta$  decay. In none of the calculations has the residual QRPA interaction ever been fully consistent with that of an underlying HFB calculation. Finally, even Ref. [13], which treats all the nucleons as active, forces them to occupy few harmonic-oscillator levels rather than continuum-like states. Here we overcome all these limitations, allowing axially symmetric deformation, using a modern and well-tested Skyrme functional for both the Hartree-Fock-Bogoliubov (HFB) mean-field calculation and the QRPA that is based on it, keeping all the nucleons active, and placing the nucleus inside a large cylindrical box, so that discretized versions of continuum states up to high energy are available.

Deformed Skyrme-QRPA calculations of this type have been applied extensively in recent years to nuclear vibrations (see e.g., [14–18]) and will soon be applied to single-beta decay [19]. Our implementation, described in detail below, is via a B-spline-based HFB code with the above-mentioned cylindrical-box boundary conditions followed by the construction and diagonalization of the QRPA Hamiltonian matrix in the basis of canonical two-quasiparticle states. The calculations consume enough CPU hours to require a supercomputer, and so we restrict ourselves here to four isotopes —  $^{76}\text{Ge}$ ,  $^{130}\text{Te}$ ,  $^{136}\text{Xe}$  and  $^{150}\text{Nd}$  — used in the some of the most promising of current or proposed experiments [20–28]. The deformation

and pairing in the initial and final nuclei are often quite different and matrix elements can be suppressed as a result [5]; our numbers depend crucially on the overlap of intermediate-nucleus states created by exciting the initial ground state with those created by exciting the final ground state. The QRPA supplies only transition amplitudes and so must be extended to obtain the overlap. Here we will apply a prescription like that in Ref. [5], while noting that a well justified and tractable expression is still lacking.

This article is organized as follows: Section II contains a brief overview of the matrix elements governing double-beta decay and of the Skyrme QRPA. Section III describes the details of our computational implementation and Sec. IV presents our results. Section V is a conclusion.

## II. DOUBLE-BETA DECAY AND THE QRPA

### A. Decay operators

The lifetime for  $0\nu\beta\beta$  decay, if there are no heavy particles mediating the decay, is

$$[T_{1/2}^{0\nu}]^{-1} = G^{0\nu} \langle m_\nu \rangle^2 |M^{0\nu}|^2, \quad (1)$$

where  $\langle m_\nu \rangle^2$  is a weighted average of three neutrino masses,  $G^{0\nu}$  is a phase space factor (recently recomputed in Ref. [29]), and  $M^{0\nu}$  is a nuclear matrix element<sup>1</sup>. Although the matrix element contains intermediate states and an energy denominator, it can to good approximation [31] be represented by one involving only the initial and final ground states. In this ‘‘closure’’ approximation and neglecting the small tensor term, one can write the matrix element as

$$M^{0\nu} = \frac{2R}{\pi(1.25)^2} \int_0^\infty q dq \quad (2)$$

$$\times \langle f | \sum_{a,b} \frac{j_0(qr_{ab}) [h_F(q) + h_{GT}(q)\vec{\sigma}_a \cdot \vec{\sigma}_b]}{q + \bar{E} - (E_i + E_f)/2} \tau_a^+ \tau_b^+ | i \rangle,$$

where the factor 1.25 is inserted by convention,  $|i\rangle$  and  $|f\rangle$  are the ground states of the initial and final nuclei,  $r_{ab} = |\vec{r}_a - \vec{r}_b|$  is the distance between nucleons  $a$  and  $b$ ,  $j_0$  is the usual

<sup>1</sup> This matrix element differs from the unprimed  $M^{0\nu}$  used elsewhere by a factor of  $g_A^2/1.25^2$ . The two are equivalent when  $g_A$  is taken to be 1.25, but differ when it is modified. (Actually [30],  $g_A$  is closer to 1.27 than 1.25, but we follow tradition here.) The convention we use puts all the  $g_A$  dependence in the matrix element and none in the phase-space factor.

spherical Bessel function,  $\bar{E}$  is an average excitation energy to which the matrix element is insensitive (and for which we use the value 10 MeV), and the nuclear radius  $R \equiv 1.2A^{1/3}$  fm is inserted with a compensating factor in the phase-space function to make the matrix element dimensionless. The “form factors”  $h_F$  and  $h_{GT}$  are given by

$$\begin{aligned} h_F(q) &\equiv -g_V^2(q^2) \\ h_{GT}(q) &\equiv g_A^2(q^2) - \frac{g_A(q^2)g_P(q^2)q^2}{3m_p} + \frac{g_P^2(q^2)q^4}{12m_p^2} \\ &\quad + \frac{g_M^2(q^2)q^2}{6m_p^2}, \end{aligned} \quad (3)$$

with

$$\begin{aligned} g_V(q^2) &= \frac{1}{(1 + q^2/(0.71 \text{ GeV}^2))^2} \\ g_A(q^2) &= \frac{1.27}{(1 + q^2/(1.09 \text{ GeV}^2))^2} \\ g_P(q^2) &= \frac{2m_p g_A(q^2)}{q^2 + m_\pi^2} \quad g_M(q^2) = 3.70g_V(q^2). \end{aligned} \quad (4)$$

Here  $m_p$  and  $m_\pi$  are the proton and pion masses.

The two-neutrino double-beta decay rate, which we will use to fit parameters for our  $0\nu\beta\beta$  calculation, can be written as

$$[T_{1/2}^{2\nu}]^{-1} = G^{2\nu} |M^{2\nu}|^2. \quad (5)$$

where  $G^{2\nu}$  is another phase-space factor (also recomputed in Ref. [29]) and  $M^{2\nu}$  is a matrix element. The closure approximation is not good for two-neutrino decay, and the matrix element must contain intermediate states explicitly:

$$M^{2\nu} \approx \sum_n \frac{\langle f | \sum_a \vec{\sigma}_a \tau_a^+ | n \rangle \langle n | \sum_b \vec{\sigma}_b \tau_b^+ | i \rangle}{E_n - (M_i + M_f)/2}, \quad (6)$$

where  $n$  labels states in the intermediate nucleus with energy  $E_n$ ,  $M_i$  and  $M_f$  are the masses of initial and final nuclei, and the effects we have neglected — forbidden currents, the Fermi matrix element, etc. — are small [32–34].

Recent study [35, 36] has shown that realistic short-range correlations have only a small effect on the double-beta matrix elements. Including them here, even approximately, would complicate our computational procedure considerably and so we omit them altogether.

## B. Deformed Charge-changing QRPA

The self-consistent axially-symmetric Skyrme-HFB-QRPA method for like-particle excitations, on which our code is based, is described thoroughly in Refs. [37], [14], and [15]. We modify the code discussed there in a rather straightforward way to work with charge-changing modes rather than like-particle modes. Obviously, we must change the basis of like-two-quasiparticle states to a basis of one-quasiproton-one-quasineutron states. We then construct the QRPA matrix given in Eqs. (A1) – (A6) of Ref. [37], with the following changes: a) we remove the Coulomb interaction, and b) we keeping only the terms in the effective particle-hole Skyrme interaction — displayed in Eq. (B13) of Ref. [37] — that contribute to the QRPA matrix elements  $A_{pn,p'n'}$  and  $B_{pn,p'n'}$ . We can do this easily by rewriting the operator  $\vec{\tau} \cdot \vec{\tau}'$  in that equation in terms of the operators “1” and  $P_\tau \equiv \frac{1}{2}(1 + \vec{\tau} \cdot \vec{\tau}')$  and then keeping only the terms containing  $P_\tau$ . Finally, we modify the part of the code that treats pairing so that it can separately produce isovector ( $S = 0$ ) and isoscalar ( $S = 1$ ) matrix elements.

We adopt the Skyrme functional (or effective interaction) SkM\* [38]; that functional has been shown to describe nuclear deformation well and reproduces low-lying quadrupole vibrations in rare-earth nuclei noticeably better than the comparably popular functional SLy4 [14]. We modify the time-odd particle-hole part of the functional as in [39], which discussed charge-changing transitions, by setting the parameters (defined in that reference)  $C_1^T = 0$ ,  $C_1^{\nabla s} = 0$ , and  $C_1^s[0] = C_1^s[\rho_{\text{nm}}] = 100 \text{ Mev fm}^3$  ( $\rho_{\text{nm}}$  is nuclear-matter density). With these modifications, the functional reproduces [19] the location of the Gamow-Teller resonance and the fraction of observable strength in the resonance. We will report results with and without the modifications to show their effect.

For the particle-particle part of the functional we use a simple volume (zero-range) pairing interaction, the strength of which we adjust separately in the isoscalar channel ( $T = 0$ ) and in each of the three isovector ( $T = 1$  with  $T_z = -1, 0$ , and 1) channels. We describe the adjustment in more detail in the next section.

Evaluating the  $0\nu\beta\beta$  matrix elements requires a multipole decomposition of  $M^{0\nu}$  suitable for cylindrical geometry. The details of that appear in the Appendix.

### III. COMPUTATIONAL IMPLEMENTATION

Only recently have fully self-consistent deformed Skyrme-QRPA calculations entered the scene. The combination of methods we use here requires many thousands of CPU hours. Our methodology will at some point be obsolete because of the development of much faster Finite Amplitude [40] and iterative Arnoldi [41] approaches, which use mean-field codes with time-independent constraints to solve the QRPA equations. Our method, by contrast, involves the explicit construction and diagonalization of the QRPA Hamiltonian matrix in a basis of two-canonical-quasiparticle states. These states are obtained from the HFB calculation mentioned previously.

To solve the initial HFB equations we use the Vanderbilt deformed HFB code [42], which represents wave functions in a basis of B-splines. Our cylindrical box has dimensions  $r_{\max} = z_{\max} = 20$  fm, about three times as large as the radius of the heaviest nucleus studied here and a number found suitable in Ref. [42]. Our mesh spacing is 0.7 fm and the energy cutoff of the HFB solutions is 60 MeV. We do not restrict the deformation (except to be axially symmetric) but rather allow the mean field to evolve freely to the nearest local binding-energy minimum. Using a range of quadrupole deformation parameters  $\beta_2$  as initial guesses, we find one or more local minima and select the most bound solution as the mean field on which we base the QRPA. In  $^{76}\text{Ge}$ , however, we do not use the most bound solution; we discuss the reasons for this exception in the next section. To obtain the strength of the proton-proton and neutron-neutron ( $T = 1, T_z = \pm 1$ ) pairing interaction we match the HFB pairing gaps with the experimental pairing gaps obtained from a three-point interpolation formula, with separation energies from the ENSDF [43] database.

The computational requirements for running our charge-changing QRPA code are significantly less than those for the like-particle code on which it is based because a) the proton-neutron two-quasiparticle basis is only about half the size of the like-two-quasiparticle basis, and b) the removal of the Coulomb interaction relieves us of a large computational burden. For a given multipole, our charge-changing code typically runs much faster than the like-particle code. That speedup, however, still leaves us with runs that consume many thousands of CPU hours per multipole in each nucleus.

We cannot include all one-quasiproton-one-quasineutron states in our QRPA basis and so truncate the same way as in Ref. [14]. The truncation is controlled by two parameters

$v_{\text{cut}}^{\text{pp}}$  and  $v_{\text{cut}}^{\text{ph}}$ . The first allows us to remove two-quasiparticle states with almost completely two-particle or two-hole nature (i.e. states that primarily lie in the  $A \pm 2$  neighbors of the reference nucleus instead of the in intermediate double-beta nucleus), and the second lets us cut out states in which one of the particles is far below the Fermi surface and the other far above it. Such excitations have very high energy and do not mix significantly with lower-energy states. In practice 15,000 two-quasiparticle states for the lowest multipoles, out of a total of about half a million, are enough to approximate the exact answer very well, making the construction and diagonalization of the QRPA matrix tractable on a supercomputer.

After diagonalizing the QRPA Hamiltonian, we need to determine the double-beta-decay matrix elements. For  $0\nu\beta\beta$  decay, the matrix element can be written as

$$M^{0\nu} = \frac{2R}{(1.25)^2\pi} \sum_{pn} \langle 0_f^+ | c_{-p}^\dagger c_n | N \rangle \sum_{NN'} \langle N | N' \rangle \quad (7)$$

$$\times \sum_{p'n'} \langle N' | c_{p'}^\dagger c_{-n'} | 0_i^+ \rangle (K_{pn,p'n'}^F + K_{pn,p'n'}^{GT}) ,$$

where  $c_k^\dagger$  are particle-creation operators, the indices with  $p$  refer to protons and those with  $n$  to neutrons, each index stands for the set of quantum numbers  $p = \{j_p^z, \pi_p, k_p\}$  (angular-momentum along on the intrinsic axis, parity, and an additional enumerating index), a minus sign in front of an index means that the sign of the  $j^z$  quantum number is reversed, and

$$K_{pn,p'n'}^F = \int_0^\infty q dq \langle pp' | \frac{j_0(qr_{12})h_F(q)}{q + \bar{E} - (E_i + E_f)/2} \tau_1^+ \tau_2^+ | nn' \rangle \quad (8)$$

$$K_{pn,p'n'}^{GT} = \int_0^\infty q dq \langle pp' | \frac{j_0(qr_{12})h_{GT}(q)\vec{\sigma}_1 \cdot \vec{\sigma}_2}{q + \bar{E} - (E_i + E_f)/2} \tau_1^+ \tau_2^+ | nn' \rangle .$$

The two-particle states in Eq. (8) are antisymmetrized. We use a multipole expansion, detailed in the Appendix, to evaluate the two-body matrix elements in Eq. (8) with B-spline integration. The coding for the two-neutrino two-body matrix elements, which we use to evaluate the matrix element in Eq. (6), requires no Bessel function expansion.

Two-neutrino decay is simpler for another reason as well; only states with angular momentum and parity  $J^\pi = 1^+$  contribute to the matrix element. In our deformed calculation we follow the usual procedure [4, 44] of representing laboratory states in a rigid-rotor approximation as combinations of a) Wigner functions  $D_{MK}^J$  and  $D_{M-K}^J$  of Euler angles, and b) an intrinsic QRPA state with a well-defined projection  $K$  along the symmetry axis of the angular momentum  $\vec{J}$ .  $M^{2\nu}$  thus gets contributions only from states with  $|K| \leq 1$ . In



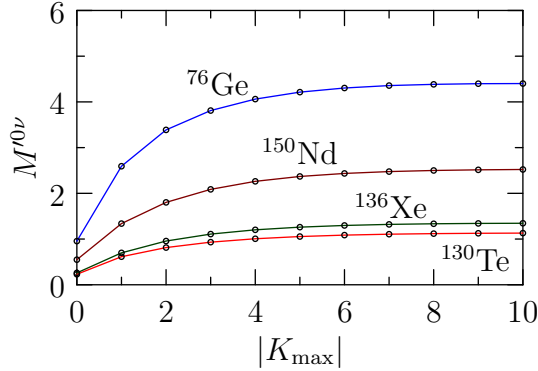


FIG. 1. (Color online.) The cumulative  $^{76}\text{Ge}$   $0\nu\beta\beta$  matrix element (using SkM\* and  $g_A = 1.0$ ) as the number of intermediate-state multipoles  $K^\pi$  is increased. Convergence is reached by  $|K| = 10$ . Both positive and negative parities are included, as are both Fermi and Gamow-Teller contributions.

neutrinoless decay, on the other hand, states with any  $K^\pi$  contribute. The contributions get progressively smaller as  $K$  gets larger. Including state with  $|K| \leq 10$  is enough to approximate the matrix element accurately, as Fig. 1 shows.

One interesting feature of Eq. (7) is the presence of the overlap  $\langle N|N'\rangle$ . The QRPA is a small-amplitude approximation and although it provides transition densities from a ground state to excited states, it can't, without extension, provide excited state wave functions. The excited states  $|N\rangle$  and  $|N'\rangle$  are based on different quasiparticle vacua and the quasiboson approximation that is inherent in the QRPA erases the information necessary to relate the two vacua. Two expressions for the overlap have been given in the past few years: one, from Ref. [5], neglects “scattering terms” even though they cannot be shown to be small and the other, laid out in Ref. [45], uses the form of the boson vacuum but replaces the bosons with the fermion pairs from which they stem. Unfortunately, this last idea leads to expressions that can only be evaluated perturbatively; these become unwieldy after the lowest couple of orders in the expansion, the convergence of which may not be fast. Here we simply evaluate the overlap in the quasi-Tamm-Dancoff approximation (neglecting the QRPA “Y” amplitudes); in this limit of the QRPA, excited states are well-defined two-quasiparticle excitations of HFB vacua and require no bosonization. The results are not very different from those obtained in the scheme proposed in Ref. [5]. We provide more details in the Appendix.

As is typical in QRPA calculations, we use the measured values of two-neutrino decay

rates to fit proton-neutron pairing strengths (which have no effect in the HFB part of the calculation because of the significant neutron excess). Following a suggestion in Ref. [46], we adjust the isovector ( $T = 1, T_z = 0$ ) strength so that the Fermi  $2\nu\beta\beta$  matrix element vanishes, as it should (almost) because the ground state of the final nucleus has a different isospin than the double-isobar-analog state of the initial nucleus. If instead we fix the proton-neutron isovector pairing strength at the average of the proton-proton and neutron-neutron pairing strengths, we find a nearly identical result. The isoscalar pairing strength, which we call  $V_0$  here, is the parameter typically called  $g_{pp}$  in other QRPA calculations. We adjust it so as to reproduce the experimental two-neutrino matrix element, with both an unquenched ( $g_A = 1.25$ , see the footnote) and quenched ( $g_A = 1.0$ ) axial-vector coupling constant. We then use the resulting pairing strengths in computing the  $0\nu\beta\beta$  matrix elements, once for each value of  $g_A$ . For  $^{130}\text{Te}$  and  $^{136}\text{Xe}$ , we compute the neutrinoless double-beta-decay matrix element with the unmodified SkM\* over a range of isoscalar pairing values  $V_0$  to assess its sensitivity to the fit. Some other authors (see, e.g., Ref. [47]) renormalize the QRPA so that the effects of proton-neutron pairing are weakened; that procedure would spoil the self-consistency of the HFB-QRPA framework and we do not adopt it here.

#### IV. RESULTS AND DISCUSSION

We start by comparing the quadrupole deformation parameters  $\beta_2$  obtained from our HFB calculation to other theoretical and experimental values in Tab. I. With the exception of  $^{76}\text{Se}$ , where our Skyrme-HFB computation fails to converge to a prolate solution, our quadrupole deformations are similar to those obtained using Sk3 and SG2 Skyrme interactions in Ref. [9]. The failure to converge is most likely due to a very flat bottom of the binding energy curve with respect to deformation in  $^{76}\text{Se}$ .

In  $^{76}\text{Ge}$ , the minimum energy occurs at a prolate deformation of  $\beta_2 = 0.18$ . This deformation is so different from that of  $^{76}\text{Se}$ , however, that our predicted two-neutrino matrix element is smaller than the measured value no matter what we use for  $g_A$  or  $V_0$ . We therefore choose to use the local near-spherical minimum ( $\beta_2 = -0.025$ ) for  $^{76}\text{Ge}$  instead. As we shall see, this gives us a result that is not too different from other QRPA numbers, including those of Ref. [6], which presents both spherical-spherical and prolate-prolate calculations. It also indicates, however, that the QRPA is inadequate in this system. The soft surfaces with

	this work	Ref. [9]		Exp.	
		Sk3	SG2	Ref. [48]	Ref. [49]
$^{76}\text{Ge}$	0.184 <sup>a</sup>	0.161	0.157	0.095(30)	0.2623(9)
$^{76}\text{Se}$	-0.018	-0.181	-0.191	0.163(33)	0.3090(37)
$^{130}\text{Te}$	0.01	-0.076	-0.039	0.035(23)	0.1184(14)
$^{130}\text{Xe}$	0.13	0.108	0.161	-	0.1837(49)
$^{136}\text{Xe}$	0.004	0.001	0.016	-	0.122(10)
$^{136}\text{Ba}$	-0.021	0.009	0.070	-	0.1258(12)
$^{150}\text{Nd}$	0.27	0.266	0.271	0.367(86)	0.2853(21)
$^{150}\text{Sm}$	0.22	0.207	0.203	0.230(30)	0.1931(21)

<sup>a</sup> -0.025 used

TABLE I. The quadrupole deformations  $\beta_2$  of the initial and final nuclei in our work, compared with the values obtained in [9] and experimental values from [48, 49]

multiple minima require a formulation that mixes mean fields, e.g. the generator-coordinate method (often referred to as energy-density functional (EDF) theory) of Ref. [50], or an extension thereof.

In the daughter nucleus  $^{130}\text{Xe}$  we get a prolate solution, making ours the first QRPA calculation to take the deformation into account in the decay of  $^{130}\text{Te}$ . The study in Ref. [51], using HFB with the Gogny interaction, finds a second minimum with oblate deformation and a barrier of only 1 MeV or so separating the two minima. As in  $^{76}\text{Se}$ , therefore, the use of a single mean-field in the construction of the  $^{130}\text{Xe}$  ground state is somewhat suspect.

We don't reproduce experimental  $Q$ -values as well as deformations, in part because the errors in the binding energies of the nuclei add in quadrature. But for the record, our HFB calculation produces  $Q = 4.84$  MeV (vs. the experimental value of 2.04 MeV) in  $^{76}\text{Ge}$ ,  $Q = 4.22$  MeV (vs. the experimental value of 2.53 MeV) in  $^{130}\text{Te}$ ,  $Q = 5.60$  MeV (vs. 2.46 MeV) in  $^{136}\text{Xe}$ , and  $Q = 2.35$  MeV (vs 3.371 MeV) in  $^{150}\text{Nd}$ . Other calculations with different Skyrme functionals produce discrepancies of the same order [52].

We turn now to the matrix elements themselves. Figure 2 displays the dependence of the

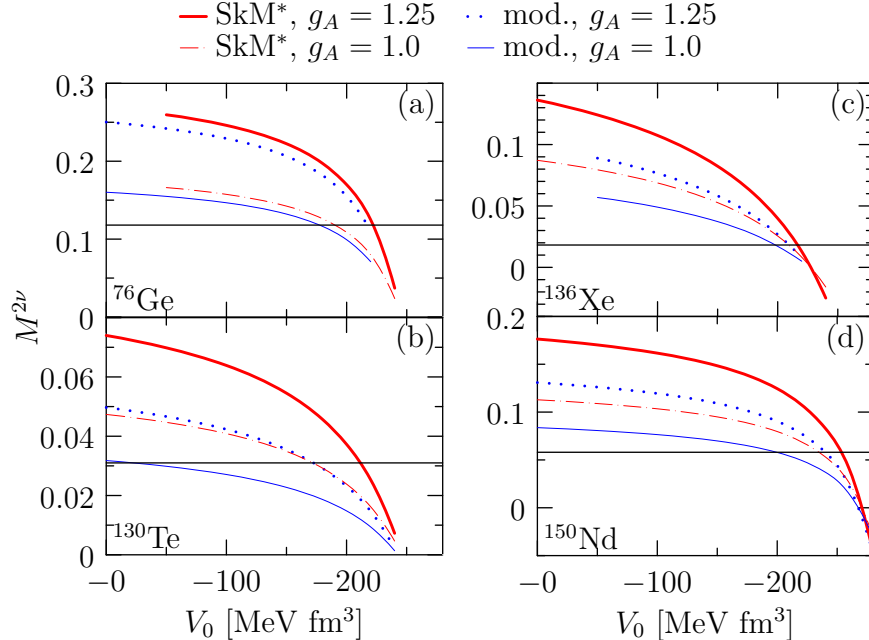


FIG. 2. (Color online.) The dependence of two-neutrino double-beta decay matrix elements on  $V_0$ , the isoscalar pairing strength. The thick solid and dashed (red) curves are produced by the original SkM\* interaction and the dotted and thin (blue) curves by the modified interaction. The thick solid and dotted curves are computed with  $g_A = 1.25$ , the dashed and thin solid curves with the quenched value  $g_A = 1.0$ .

$2\nu\beta\beta$  matrix element on the isoscalar pairing strength  $V_0$  in the four systems we study. We use the recent evaluation of the phase-space factors in Ref. [29] to extract the experimental matrix elements. Because  $M^{2\nu}$  for  $^{136}\text{Xe}$  was just measured for the first time by the EXO-200 [53] and KamLAND-Zen [24] experiments, ours is the first QRPA double beta decay computation to use an experimentally obtained value rather than an upper limit to determine the strength of isoscalar pairing.

Figure 3 illustrates the dependence of the  $0\nu\beta\beta$  decay matrix element on  $V_0$ . The neutrinoless matrix element is less sensitive to this pairing mode than the two-neutrino matrix element. We collect our final results for the  $0\nu\beta\beta$  matrix elements with both  $g_A = 1.25$  and  $g_A = 1.0$  in Table II. The modification of SkM\* usually suppresses the  $0\nu\beta\beta$  matrix element, by up to 15%. It actually seems to increase the matrix element in  $^{130}\text{Te}$  by 17% for  $g_A = 1.0$ , but as Fig. 2 shows, the fitting procedure for  $V_0$  with  $g_A = 1.0$  gives an anomalously small value, and so that result must be taken with a grain of salt. In Table III we compare our

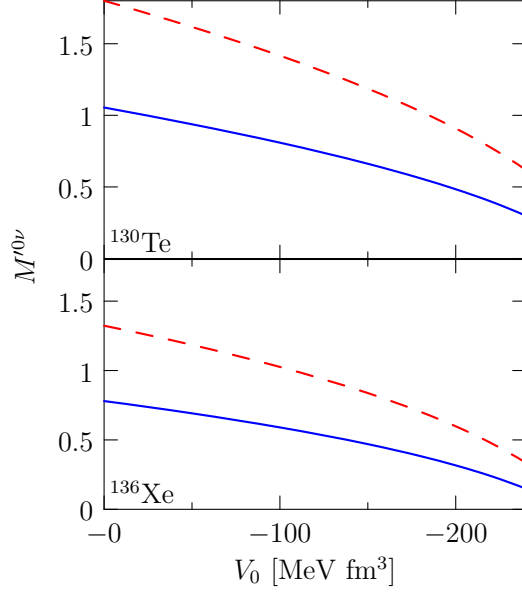


FIG. 3. (Color online.) The dependence of  $M^{0\nu}$  in  $^{136}\text{Xe}$  and  $^{130}\text{Te}$  on the  $V_0$  produced by the unmodified SkM\* interaction. The solid curve represents the results with  $g_A = 1.0$  and the dashed curve represents the results with  $g_A = 1.25$ .

values with the modified SkM\* and  $g_A = 1.25$  with earlier theoretical results. Our matrix elements for  $^{76}\text{Ge}$  and  $^{150}\text{Nd}$  are in a good agreement with the spherical result for Ge and the deformed one for Nd in Ref. [6]. For  $^{136}\text{Xe}$  and  $^{130}\text{Te}$  we get noticeably smaller matrix elements than obtained in prior work, all of which was carried out in the spherical QRPA. Figure 4 displays the same information as the table graphically.

The suppression we see in  $^{130}\text{Te}$  can be attributed to the deformation of the daughter

	SkM*		modified SkM*	
	$g_A = 1.0$	$g_A = 1.25$	$g_A = 1.0$	$g_A = 1.25$
$^{76}\text{Ge}$	4.40	5.53	4.12	5.09
$^{130}\text{Te}$	1.13	1.38	1.32	1.37
$^{136}\text{Xe}$	1.26	1.68	1.18	1.55
$^{150}\text{Nd}$	2.52	3.14	2.14	2.71

TABLE II. The  $0\nu\beta\beta$  matrix elements in our Skyrme-HFB-QRPA calculation, with both the functional SkM\* and a modified version of it, and with both a quenched and unquenched axial-vector coupling constant  $g_A$ .

	present	QRPA/T	QRPA/J	ISM	IBM-2	PHFB	EDF
$^{76}\text{Ge}$	5.09	5.30, 4.69*	5.355	2.96	5.465	—	4.60
$^{130}\text{Te}$	1.37	4.92	4.221	2.81	4.059	4.66	5.13
$^{136}\text{Xe}$	1.55	3.11	2.802	2.32	2.220	—	4.20
$^{150}\text{Nd}$	2.71	3.34*	—	—	2.321	3.24	1.71

TABLE III. Comparison of our  $0\nu\beta\beta$  matrix elements, from the modified SkM\* functional and  $g_A = 1.25$ , with those obtained from the interacting shell model (ISM, [54]), QRPA calculations by the Tübingen group [6, 35] (QRPA/T) and Jyväskylä group [55] (QRPA/J), the energy-density-functional method [50] (EDF), projected HFB [56] (PHFB) and the interacting boson model [57] (IBM-2). Prior results that include deformation are indicated by a star.

nucleus. Previous QRPA calculations for  $^{130}\text{Te}$  [35, 55] have assumed spherical symmetry. We've already mentioned, however, that a single minimum may not be adequate to represent the ground state of  $^{130}\text{Xe}$ . We suspect that the complete neglect of deformation in previous work leads to a matrix element that is too large, but it may also be that our sharp prolate Xe ground state yields one that is too small.

The other decay in which we disagree significantly with previous QRPA calculations is that of  $^{136}\text{Xe}$ . Our significantly smaller result here is not caused by deformation difference, nor does it come from the availability of new two-neutrino decay data. Instead, it can be traced to the overlap between the initial and final HFB mean fields. This overlap usually reflects the difference in deformation between the mother and daughter nuclei, and for that reason, has been completely neglected in previous QRPA calculations for the decay of  $^{136}\text{Xe}$ , where both the initial and final nuclei are spherical. We find here, however, that differences in pairing structure in the neutron mean fields lead to a small overlap:  $\langle \text{HFB}_f | \text{HFB}_i \rangle = 0.47$ . The suppression is related to the  $N = 82$  shell closure, which produces a sharp Fermi surface that smooths measurably with the addition of two neutrons. We see no reason to completely neglect the overlap, but the situation may be analogous to that in the decay of  $^{130}\text{Te}$ . A more realistic representation of pairing than is offered by the HFB mean field might make the difference in structure between the initial and final nuclei a little less dramatic. Interestingly, a recent shell-model [58] calculation finds that increasing the model-space size produces the smallest matrix element yet for this decay: 1.46.

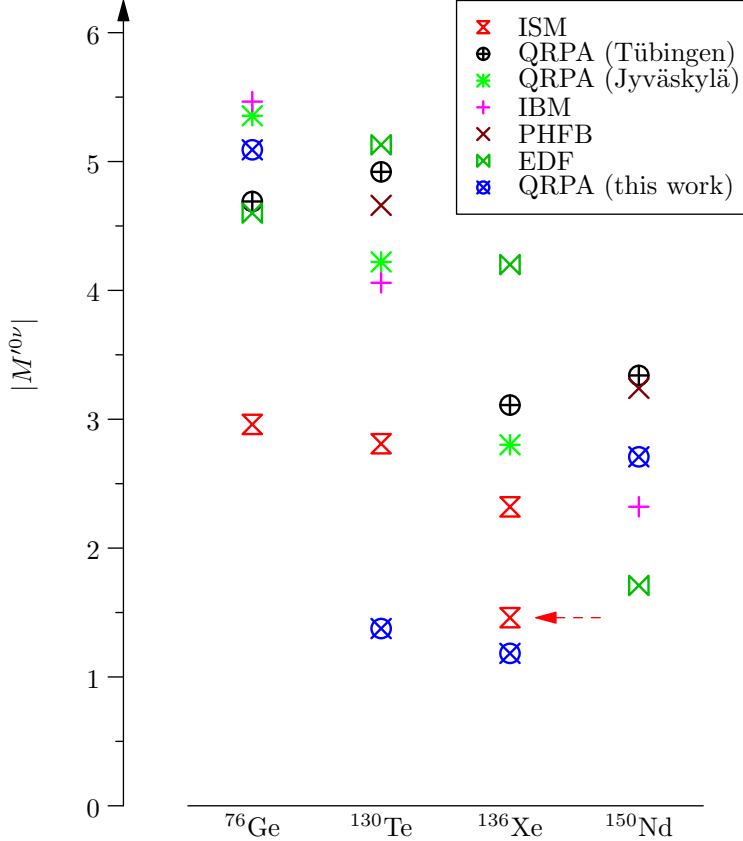


FIG. 4. (Color online.) The results of Table III for  $g_A = 1.25$ . The dashed (red) arrow points to the new shell-model result of Ref. [58] in  $^{136}\text{Xe}$ .

All the substantial differences between our QRPA calculations and others can be traced to deformation or pairing effects that were neglected in previous work. Our use of a self-consistent QRPA with all nucleons treated as active participants, the continuum accounted for, etc., doesn't, in itself, change results dramatically. That finding is not altogether surprising. Self-consistency is important in the QRPA partly because it eliminates spurious strength. In the charge changing QRPA, however, the absence of proton-neutron mixing in the HFB and the explicit breaking of isospin mean that there is no spurious strength even in non-self-consistent calculations. More importantly, it is already well known [59] that differences between variants of the QRPA largely disappear when the strength of the isoscalar pairing interaction is adjusted so that each variant reproduces the measured two-neutrino rate. Our variant does not escape this fate; that one parameter is a like a broad and coarse brush that paints over any sophistication in the underlying method.

## V. CONCLUSIONS

We have performed large-scale Skyrme-HFB-QRPA computations for four important double-beta emitters. We have allowed for axial deformation of the initial and final nuclei. Our implementation increases the scale of the computation to the limits of contemporary technology.

For  $^{76}\text{Ge}$  and the very deformed  $^{150}\text{Nd}$ , our results are in line with the earlier results of Ref. [6]. We note, however, that the assumption both here and elsewhere that the  $^{76}\text{Ge}$  and  $^{76}\text{Se}$  ground states are spherical probably results in a matrix element that is too large.

In  $^{130}\text{Te}$  we improved on the ground state used in previous QRPA calculations by taking into account the deformation of the final nucleus. Shape coexistence in the daughter  $^{130}\text{Xe}$  is beyond the scope of the QRPA, however; if present, it could further modify the value of the matrix element.

Our  $^{136}\text{Xe}$  matrix element is the first QRPA result obtained from the new two-neutrino-decay measurements. It is also the first to take into account the overlap of the two sets of QRPA intermediate states. The overlap is smaller than one might expect because of the sharp neutron Fermi surface in the initial nucleus. In reality, the Fermi surface cannot be perfectly sharp, and the true matrix element is probably not suppressed quite this much. The recent shell-model result for this matrix element [58], however, imply that past computations may have overestimated the  $^{136}\text{Xe}$  double beta decay rate.

Our computation demonstrates that there is little to be gained by further increasing the size and sophistication of QRPA calculations. Any straightforward alterations to the QRPA, other than the development of a better energy-density functional, are unlikely to improve the results substantially. We have reached the point at which shortcomings of the QRPA itself restrict improvement. The inability to treat shape coexistence is an issue at least for the daughter nuclei  $^{76}\text{Se}$  and  $^{130}\text{Xe}$ . The mean-field treatment of pairing may be a problem in nuclei such as  $^{136}\text{Xe}$  that have closed shells. We can address these issues only by moving beyond the QRPA.



## ACKNOWLEDGMENTS

Support for this work was provided through the Scientific Discovery through Advanced Computing (SciDAC) program funded by U.S. Department of Energy, Office of Science, Advanced Scientific Computing Research and Nuclear Physics, under award number DE-SC0008641, and by the UNEDF SciDAC Collaboration under DOE grants DE-FC02-07ER41457 and DE-FC02-09ER41584. One of us (M.T.M.) gratefully acknowledges fruitful discussions with Prof. Mihai Horoi, alongside the support and hospitality he extended at Central Michigan University during the spring of 2012.

This work used the Extreme Science and Engineering Discovery Environment (XSEDE), which is supported by National Science Foundation grant number OCI-1053575. Most of the computations were performed on Kraken at the National Institute for Computational Sciences (<http://www.nics.tennessee.edu/>). This research also used resources of the National Energy Research Scientific Computing Center, which is supported by the Office of Science of the U.S. Department of Energy under Contract No. DE-AC02-05CH11231.

## Appendix: Neutrinoless double beta decay matrix elements in the cylindrical box

Equation (7) is in essence a trace of a product of four large square matrices. The transition densities in that equation are

$$\langle 0_f^+ | c_{-p}^\dagger c_n | N \rangle = s_p v_p u_n X_{pn}^N + u_p s_n v_n Y_{-p-n}^N, \quad (\text{A.1})$$

and

$$\langle N' | c_{p'}^\dagger c_{-n'} | 0_i^+ \rangle = -u_{p'} s_{n'} v_{n'} X_{p'n'}^{N'} - s_{p'} v_{p'} u_{n'} Y_{p'n'}^{N'}. \quad (\text{A.2})$$

Here the indices  $p$  and  $p'$  indicate protons, and  $n$  and  $n'$  neutrons, as discussed in the main text;  $c_p^\dagger$  is a proton creation operator, and  $u_p$  and  $s_p v_p$  are the proton occupation amplitudes in the canonical basis, in the notation of Ref. [44].  $X_{pn}^N$  and  $Y_{-p-n}^N$  are forward-going and backward-going QRPA amplitudes.

To reduce the number of nested numerical integrals in the  $0\nu\beta\beta$  matrix elements in Eq. (7), we take advantage of the following expansion for the spherical Bessel function in Eq. (8):

$$j_0(qr_{ab}) = 4\pi \sum_{l=0}^{\infty} j_l(qr_a) j_l(qr_b) \sum_{m=-l}^l Y_{lm}^*(\hat{r}_a) Y_{lm}(\hat{r}_b). \quad (\text{A.3})$$

This allows us to separate the integrals over coordinates of the two nucleons:

$$\begin{aligned}
K_{pn,p'n'}^F &= \int_0^\infty dq \frac{qh_F(q^2)}{q + E_{\text{ave}}} \sum_{l=K}^\infty (2l+1) \frac{(l-K)!}{(l+K)!} \\
&\quad \times I_{-pn}^{lK}(q) I_{p'-n'}^{lK}(q),
\end{aligned} \tag{A.4}$$

and

$$\begin{aligned}
K_{pn,p'n'}^{GT} &= \int_0^\infty dq \frac{qh_{GT}(q^2)}{q + E_{\text{ave}}} \sum_{\mu=-1}^1 (-1)^\mu \\
&\quad \times \sum_{l=\max(0,K-\mu)}^\infty (2l+1) \frac{(l-(K-\mu))!}{(l+(K-\mu))!} \\
&\quad \times I_{-pn}^{l,K-\mu,-\mu}(q) I_{p'-n'}^{l,K-\mu,\mu}(q),
\end{aligned} \tag{A.5}$$

where  $E_{\text{ave}} = \bar{E} - (E_i + E_f)/2$ . Naturally, the infinite summations over  $l$  must be truncated. For most values of the neutrino energy  $q$ , not many terms are needed for convergence. In the program we truncate the expansion dynamically by requiring a preset accuracy in the quadrature for each value of  $q$ .

The axial symmetry of the normalized canonical single-particle wave functions means that they can be written in the form

$$\Psi_a(\vec{r}) = \frac{1}{\sqrt{2\pi}} \sum_{s=\pm 1/2} \psi_a(s; \rho, z) e^{i(j_a^z - s)\phi} \chi_s, \tag{A.6}$$

where  $s$  is the spin projection,  $\chi_s$  is a standard two-component spinor, and  $j_a^z$  the angular-momentum projection onto the intrinsic axis. The integrations over the azimuthal angle  $\phi$  are trivial and the integrals  $I_{ab}^{lm}(q)$  and  $I_{ab}^{lm\nu}(q)$  are therefore only two-dimensional:

$$\begin{aligned}
I_{ab}^{lm}(q) &= \int_{-\infty}^\infty dz \int_0^\infty d\rho \rho \psi_a^\dagger(\rho, z) \psi_b(\rho, z) \\
&\quad \times j_l(q\sqrt{\rho^2 + z^2}) P_l^m \left( \frac{z}{\sqrt{\rho^2 + z^2}} \right),
\end{aligned} \tag{A.7}$$

and

$$\begin{aligned}
I_{ab}^{lm\nu}(q) &= \int_{-\infty}^\infty dz \int_0^\infty d\rho \rho \psi_a^\dagger(\rho, z) \sigma_\nu \psi_b(\rho, z) \\
&\quad \times j_l(q\sqrt{\rho^2 + z^2}) P_l^m \left( \frac{z}{\sqrt{\rho^2 + z^2}} \right).
\end{aligned} \tag{A.8}$$

Here the  $P_l^m(x)$  are the usual associated Legendre polynomials,  $\sigma_\nu$  are the Pauli matrices in the spherical vector basis and

$$\psi_a(\rho, z) = \begin{pmatrix} \psi_a(+1/2; \rho, z) \\ \psi_a(-1/2; \rho, z) \end{pmatrix}. \quad (\text{A.9})$$

As discussed in the main body of the text, we also need to evaluate the overlaps  $\langle N|N' \rangle$  between the QRPA states stemming from different mean fields. A satisfactory expression for these is lacking, but the chief ingredient in any such expression will be the overlap of two HFB vacua. The generalized Thouless theorem [44] relating the two non-orthogonal quasiparticle vacua  $|\text{HFB}_i\rangle$  (initial state) and  $|\text{HFB}_f\rangle$  (final state) to each other is:

$$|\text{HFB}_i\rangle = \mathcal{N}^{-1} \exp\left(\sum_{kl} D_{kl} a_k^{(f)\dagger} a_l^{(f)\dagger}\right) |\text{HFB}_f\rangle, \quad (\text{A.10})$$

where the  $a_k^{(f)\dagger}$  are quasiparticle creation operators in the final nucleus. The normalization factor is related to the transformation coefficients  $D_{kl}$  via the Onishi formula:

$$\mathcal{N} = \langle \text{HFB}_f | \text{HFB}_i \rangle^{-1} = \sqrt{\det(1 + D^\dagger D)}. \quad (\text{A.11})$$

Because the canonical-basis wave functions form a complete set, there exists a linear transformation between the two HFB solutions:

$$a_k^{(f)\dagger} = \sum_n (\mathcal{R}_{kn} a_n^{(i)\dagger} + \mathcal{S}_{k,-n} a_{-n}^{(i)}), \quad (\text{A.12})$$

where

$$\mathcal{R}_{kn} = \langle n|k \rangle (u_k u_n + s_k v_k s_n v_n), \quad (\text{A.13})$$

and

$$\mathcal{S}_{k,-n} = \langle n|k \rangle (u_k s_n v_n - s_k v_k u_n). \quad (\text{A.14})$$

Substituting Eq. (A.10) and (A.12) into the definition of the quasiparticle vacuum

$$a_{-k}^{(f)} |\text{HFB}_f\rangle = 0, \quad (\text{A.15})$$

expanding the exponential, and comparing the terms containing one quasiparticle creation operator, we get the matrix equation

$$\mathcal{R}^* D = -\mathcal{S}^*, \quad (\text{A.16})$$

from which we can obtain the transformation coefficients  $D_{kl}$ .

As mentioned earlier, we approximate the QRPA overlaps states by QTDA overlaps, i.e. by neglecting the  $Y$ 's. This leads finally to the expression

$$\langle N|N'\rangle = \mathcal{N}^{-1} \sum_{pn} \sum_{p'n'} X_{pn}^{N*} X_{p'n'}^{N'} \left( \mathcal{R}_{p'p} + \sum_{p''} \mathcal{S}_{p'p''} D_{p''p} \right) \left( \mathcal{R}_{n'n} + \sum_{n''} \mathcal{S}_{n'n''} D_{n''n} \right). \quad (\text{A.17})$$

This formula differs slightly from the one presented in Ref. [5] and used in most QRPA double-beta-decay calculations. Our overlap differs in that we keep the transformation between the two HFB bases accurate and neglect the usually tiny term proportional to two  $Y$  amplitudes. In test calculations we find the numerical difference between the two prescriptions to be negligible, as the common leading term is already a good approximation. A more consistent evaluation of these overlaps that includes ground-state correlations can easily get both very complicated and computationally demanding, as evidenced by recent work in the like-particle QRPA in Ref. [45].

- 
- [1] F. T. Avignone III, S. R. Elliott, and J. Engel, *Rev. Mod. Phys.* **80**, 481 (2008).
  - [2] J. D. Vergados, H. Ejiri, and F. Šimkovic, *Rep. Prog. Phys.* **75**, 106301 (2012).
  - [3] A. S. Barabash, *J. Phys. G: Nucl. Part. Phys.* **39**, 085103 (2012).
  - [4] M. S. Yousef, V. Rodin, A. Faessler, and F. Simkovic, *Phys. Rev. C* **79**, 014314 (2009).
  - [5] F. Šimkovic, L. Paceaescu, and A. Faessler, *Nuclear Physics A* **733**, 321 (2004).
  - [6] D.-L. Fang, A. Faessler, V. Rodin, and F. Simkovic, *Phys. Rev. C* **83**, 034320 (2011).
  - [7] O. Moreno, R. Alvarez-Rodriguez, P. Sarriguren, E. Moya de Guerra, F. Simkovic, and A. Faessler, *J. Phys. G* **36**, 015106 (2009).
  - [8] O. Moreno, R. Alvarez-Rodriguez, P. Sarriguren, E. Moya de Guerra, J. M. Udias, and J. R. Vignote, *Phys. Rev. C* **74**, 054308 (2006).
  - [9] R. Álvarez-Rodríguez, P. Sarriguren, E. Moya de Guerra, L. Paceaescu, A. Faessler, and F. Šimkovic, *Phys. Rev. C* **70**, 064309 (2004).
  - [10] L. Paceaescu, V. Rodin, F. Simkovic, and A. Faessler, *Phys. Rev. C* **68**, 064310 (2003).
  - [11] A. Bobyk, W. A. Kaminski, and F. Šimkovic, *Phys. Rev. C* **63**, 051301R (2001).

- [12] M. Cheoun, A. Bobyk, A. Faessler, F. Simkovic, and G. Teneva, Nucl. Phys. A **564**, 329 (1993).
- [13] C. De Conti, F. Krmpotić, and B. Vern Carlson, (2012), arXiv:1202.3511.
- [14] J. Terasaki and J. Engel, Phys. Rev. C **82**, 034326 (2010).
- [15] J. Terasaki and J. Engel, Phys. Rev. C **84**, 014332 (2011).
- [16] K. Yoshida and T. Nakatsukasa, Phys. Rev. C **83**, 021304(R) (2011).
- [17] S. Péru, G. Gosselin, M. Martini, M. Dupuis, S. Hilaire, and J.-C. Devaux, Phys. Rev. C **83**, 014314 (2011).
- [18] K. Yoshida and N. V. Giai, Phys. Rev. C **78**, 064316 (2008).
- [19] T. Shafer and J. Engel, Unpublished.
- [20] F. Bellini *et al.*, Astropart. Phys. **33**, 169 (2010).
- [21] The GERDA Collaboration, J. Phys. G: Nucl. Part. Phys. **40**, 035110 (2013).
- [22] D. G. Phillips II *et al.* (The MAJORANA Collaboration), J. Phys.: Conf. Ser. **381**, 012044 (2012).
- [23] M. Auger *et al.*, Phys. Rev. Lett. **109**, 032505 (2012).
- [24] A. Gando *et al.* (KamLAND-Zen Collaboration), Phys. Rev. C **85**, 045504 (2012).
- [25] H. Ohsumi, J. Phys.: Conf. Ser. **120**, 052054 (2008).
- [26] C. Kraus and S. J. M. Peeters, Prog. Part. Nucle. Phys. **64**, 273 (2010).
- [27] F. Sánchez, Nucl. Phys. B (Proc. Suppl.) **198**, 71 (2009).
- [28] N. Ishihara, T. Ohama, and Y. Yamada, Nucl. Inst. Meth. Phys. Res. A **373**, 32 (1996).
- [29] J. Kotila and F. Iachello, Phys. Rev. C **85**, 034316 (2012).
- [30] J. Beringer *et al.* (Particle Data Group), Phys. Rev. D **86**, 010001 (2012).
- [31] G. Pantis and J. Vergados, Phys. Lett. B **242**, 1 (1990).
- [32] W. C. Haxton and G. J. Stephenson Jr., Prog. Part. and Nucl. Phys. **12**, 409 (1984).
- [33] O. Civitarese and J. Suhonen, Nucl. Phys. A **607**, 152 (1996).
- [34] F. Simkovic, Czech J. Phys. B **38**, 371 (1988).
- [35] F. Šimkovic, A. Faessler, H. Mütter, V. Rodin, and M. Stauf, Phys. Rev. C **79**, 055501 (2009).
- [36] J. Engel and G. Hagen, Phys. Rev. C **79**, 064317 (2009).
- [37] J. Terasaki, J. Engel, M. Bender, J. Dobaczewski, W. Nazarewicz, and M. Stoitsov, Phys. Rev. C **71**, 034310 (2005).

- [38] J. Bartel, P. Quentin, M. Brack, C. Guet, and H.-B. Håkansson, Nucl. Phys. A **386**, 79 (1982).
- [39] M. Bender, J. Dobaczewski, J. Engel, and W. Nazarewicz, Phys. Rev. C **65**, 054322 (2002).
- [40] P. Avogadro and T. Nakatsukasa, Phys. Rev. C **84**, 014314 (2011).
- [41] J. Toivanen, B. G. Carlsson, J. Dobaczewski, K. Mizuyama, R. R. Rodriguez-Guzman, P. Toivanen, and P. Vesely, Phys. Rev. C **81**, 034312 (2010).
- [42] E. Terán, V. E. Oberacker, and A. S. Umar, Phys. Rev. C **67**, 064314 (2003).
- [43] “Evaluated Nuclear Structure Data File (ENSDF),” <http://www.nndc.bnl.gov/ensdf/>.
- [44] P. Ring and P. Schuck, *The Nuclear Many-Body Problem*, Texts and Monographs in Physics (Springer, 2004).
- [45] J. Terasaki, Phys. Rev. C **86**, 021301(R) (2012).
- [46] V. Rodin and A. Faessler, Phys. Rev. C **84**, 014322 (2011).
- [47] J. Schwieger, F. Simkovic, and A. Faessler, Nucl. Phys. A **600**, 179 (1996).
- [48] G. A. Lalazissis, S. Raman, and P. Ring, At. Data Nucl. Data Tables **71**, 1 (1999).
- [49] S. Raman, C. W. Nestor, Jr., and P. Tikkanen, At. Data Nucl. Data Tables **78**, 1 (2001).
- [50] T. R. Rodríguez and G. Martínez-Pinedo, Phys. Rev. Lett. **105**, 252503 (2010).
- [51] L. M. Robledo, R. R. Rodríguez-Guzmán, and P. Sarriguren, Phys. Rev. C **78**, 034314 (2008).
- [52] J. Dobaczewski, M. Stoitsov, and W. Nazarewicz, AIP Conference Proceedings **76**, 51 (2004), arXiv:nucl-th/0404077.
- [53] N. Ackerman *et al.* (EXO Collaboration), Phys. Rev. Lett. **107**, 212501 (2011).
- [54] J. Menéndez, A. Poves, E. Caurier, and F. Nowacki, Nucl. Phys. A **818**, 139 (2009).
- [55] J. Suhonen and M. Kortelainen, Int. J. Mod. Phys. E **17**, 1 (2008).
- [56] P. K. Rath, R. Chandra, K. Chaturvedi, P. K. Raina, and J. G. Hirsch, Phys. Rev. C **82**, 064310 (2010).
- [57] J. Barea and F. Iachello, Phys. Rev. C **79**, 044301 (2009).
- [58] M. Horoi and B. A. Brown, (2013), arXiv:1301.0256.
- [59] V. A. Rodin, A. Faessler, F. Šimkovic, and P. Vogel, Phys. Rev. C **68**, 044302 (2003).